Journal of Catalysis **187,** 238–244 (1999)
Article ID jcat.1999.2612, available online at http://www.idealibrary.com on IDEAL®

Chemisorption of Methane on Ni(100) and Ni(111) Surfaces with Preadsorbed Potassium

Hanne S. Bengaard,* Ib Alstrup,† Ib Chorkendorff,*,‡ Sven Ullmann,† Jens R. Rostrup-Nielsen,† and Jens K. Nørskov‡

*Interdisciplinary Research Center for Catalysis (ICAT) and ‡Center for Atomic-Scale Materials Physics (CAMP), Physics Department, Building 307, Technical University of Denmark, DK-2800 Lyngby, Denmark; and †Haldor Topsøe Research Laboratories, Nymøllevej 55, DK-2800 Lyngby, Denmark
E-mail: ia@topsoe.dk

Received April 27, 1999; revised June 22, 1999; accepted June 22, 1999

Dissociative chemisorption of methane on Ni(100) and Ni(111) surfaces with preadsorbed potassium in the coverage range 0–0.12 monolayer (ML) has been measured at 475 and 500 K. The results show that the methane sticking probability is strongly diminished by the presence of potassium. An explanation for this surprising inhibition has been sought by performing large-scale density functional theory calculations of the dissociative chemisorption of methane on Ni(100) and Ni(111) surfaces with and without preadsorbed potassium. The calculations show that the barrier for dissociation of methane is increased by about 0.2 eV when 0.125 ML potassium is preadsorbed on both nickel surfaces. In the transition state of the dissociating methane molecule a dipole moment is induced. It is shown that the increase of the barrier is largely given by the interaction between the induced dipole moment in the transition state and the electrostatic field induced by the potassium adatoms.
© 1999 Academic Press

1. INTRODUCTION

The chemisorption of methane on transition metal surfaces has attracted much attention in recent years. From a technological point of view a major motivation for this interest is that the chemisorption of CH_4 is the rate-determining step in the catalytic transformation (reforming) of the main component of natural gas into a mixture of hydrogen and carbon monoxide (syngas). Hydrogen and syngas are very important feedstocks for the larger part of the chemical industry. The mechanism of the strongly activated chemisorption of methane on transition metals is also from a scientific point of view of great current interest and has been studied and discussed in several papers (1–8). Industrially the most common way of transforming methane into syngas is through the steam or carbon dioxide reforming reactions (9), which are usually carried out by means of nickel catalysts. The performance of supported transition metal catalysts is often improved by adding other elements or compounds, so-called promoters. Very often alkali metals, usually potassium, are added to nickel steam reforming catalysts (9). It is found that the addition of alkali can suppress the reactions leading to carbon formation, which must be avoided because it can destroy the catalyst particles and block the reactor. Kinetic studies have indicated that the adsorption of steam on the catalyst support is enhanced by the presence of alkali and it is speculated that spillover of steam or OH groups to the nickel particles may play an important role (9).

Alkali metals or alkali compounds are used as important catalyst promoters for many other reactions and this has motivated numerous studies of the chemisorption of a range of molecules such as H_2, N_2, CO, NO, H_2O, and CO_2 on a number of metals with preadsorbed alkali metal atoms. Most of these studies are described in recent reviews (10–14). The mechanism of the promotion or poisoning of the chemisorption and reaction of various molecules, in particular, CO, N_2, and H_2O, by alkali adatoms has been discussed in several papers (15–17). However, very little information about the impact of preadsorbed alkali atoms on the chemisorption of methane on transition metal surfaces is available in the literature. In an account of molecular beam studies of the chemisorption of methane on Ni(111), Ceyer *et al.* (18) briefly mention that preadsorbed potassium has no influence on the chemisorption of methane on Ni(111). This remark is quite surprising for two reasons. First, it is known that the addition of alkali to the nickel catalyst decreases the steam reforming rate strongly (9, 19). Second, significant reactivity changes due to alkali have been observed for all other transition metal chemisorption systems for which the influence of alkali has been investigated (10–14).

In the present paper we report and discuss measurements of methane chemisorption at 475 and 500 K on Ni(100) and Ni(111) with preadsorbed potassium as well as density functional theory (DFT) calculations of the activation barrier for the dissociative chemisorption of methane on Ni(100) and Ni(111) surfaces with and without preadsorbed

0021-9517/99 $30.00
Copyright © 1999 by Academic Press
All rights of reproduction in any form reserved.

potassium. The experimental results show that preadsorbed potassium has a significant inhibiting influence on the chemisorption of methane on nickel. The DFT calculations show that the barriers for the dissociative chemisorption of methane on Ni(100) and Ni(111) strongly increase when 0.125 monolayer (ML) of potassium is preadsorbed. They also show that a significant dipole moment is induced when the CH_4 molecule approaches the surface and that the interaction of this dipole with electrical field from the potassium can explain the increase of the barrier.

2. EXPERIMENTAL

The experiments were carried out in an UHV system, described previously (4), with two UHV chambers. One chamber is equipped with facilities for X-ray photoelectron spectroscopy (XPS) and temperature-programmed desorption (TPD) and the second, for low energy electron diffraction (LEED). The second chamber is also equipped with an ion sputter gun, a commercial potassium source (SAES), and connections to a gas inlet system. The XPS facility is essentially identical to the standard VG ESCA 3 spectrometer. A Balzers quadrupole mass spectrometer, type QMG 420 C, is used for the TPD experiments. LEED patterns are recorded by means of reverse view LEED optics, Model RVL 6-120 (Princeton Research Instruments Inc.). Very pure gases, methane and argon (Alphagaz, >99.9999%), were used. The gases were further purified by passing through an activated nickel catalyst and the cleanliness of the gas was tested as described previously (4). The methane exposures were made by rapidly backfilling the second chamber to the desired pressure, which was measured with a capacitance pressure gauge (MKS baratron). Nielsen *et al.* (20) reported that during exposure a well-defined methane temperature equal to the sample temperature can be obtained either by using a gas pressure equal to or larger than 3 mbar or by using a thermal finger. The second chamber was fitted with such a thermal finger, which was used when small exposures were required. It consists of a copper cylinder (diameter 34 mm) with a built-in heating element and thermocouple and mounted on a linear motion device.

2.1. Cleaning of the Crystal

The nickel crystal slabs (diameter 10 mm, thickness 2 mm) with (100) and (111) surface orientations ($\pm 0.5^\circ$) were cleaned by cycles of high-temperature oxidation and reduction followed by argon ion sputtering at 1373 K. The temperature of the crystal was measured with a chromel/alumel thermocouple spot-welded to the backside of the crystal. After many cycles and a subsequent brief annealing at 1100 K, the coverage of impurities was finally below the limit of detectability ($\sim$0.01 ML) (1 ML $= 1.61 \times 10^{19}$ atoms m^{-2} for the Ni(100) and 1.85×10^{19} atoms m^{-2} for the Ni(111) surface, respectively).

2.2. Determination of Coverages

The amounts of carbon, potassium, and oxygen on the sample surface before and after adsorption were monitored by means of XPS using Al $K\alpha$ radiation from a dual anode. A relatively large pass energy of the analyzer, 100 eV, has been used during data acquisition because high signal/noise ratio is more important than high-energy resolution in the present studies. The XPS peak area ratios of the C 1*s* and the K 2*s* peaks to the Ni 3*p* peak, $R_{C,Ni}$ and $R_{K,Ni}$, were used for the determination of the carbon and potassium coverages, respectively. The areas of the XPS peaks were determined after subtraction of a nonlinear background using the algorithm suggested by Shirley (21). Although this method is based on a model, which has been shown not to be physically correct (22), it gives satisfactory results when used for a limited energy region covering one peak (23). By consistently using the same region in all the area determinations for the same peak, the ratios $R_{C,Ni}$ and $R_{K,Ni}$ give reasonably accurate, relative measures of the carbon and potassium coverages, respectively. The factor used for the conversion of the $R_{C,Ni}$ ratio into coverage was determined by measuring the XPS ratio after C saturation of the surface by chemisorption of CH_4 and C_2H_4 at temperatures $\geq$425 K. The surface structures of Ni(100) and Ni(111) saturated with carbon are *p4g* (24) and $c(5\sqrt{3} \times 9)$rec (25) corresponding to carbon coverages of 0.5 and 0.44 ML, respectively. The conversion factors for potassium were determined by adjusting the K coverage to obtain sharp LEED patterns corresponding to the $c(4 \times 2)$ Ni(100)–K structure (26) and the $p(2 \times 2)$ Ni(111)–K structure (27). Both structures correspond to a potassium coverage of 0.25 ML. Unfortunately, the Al $K\alpha_{3,4}$ satellite of the K 2*p* peak coincides with the C 1*s* peak, which gives a false carbon coverage contribution approximate of the same size as the potassium coverage. We correct for this contribution by subtracting the carbon peak area, measured after potassium deposition on the clean surface and before CH_4 exposures, from the carbon peak areas measured after each methane exposure.

2.3. Procedure

Before each series of CH_4 chemisorption measurements, the crystal was cleaned by argon ion sputtering at 975 K followed by annealing at 1100 K, deposition of potassium, and another annealing at 550 K. The temperature of the crystal was then kept constant (475 or 500 K) and the chamber was rapidly backfilled with CH_4 to the selected pressure. The exposure was finished by rapidly pumping down. The coverages were determined by XPS measurements. Exposures and coverage determinations were continued until a sufficient number of points were obtained to determine the initial sticking probability by model fitting. In some cases the exposure steps were continued close to carbon saturation of the surface. Exposure times were always 1 min or more

in order to minimize the exposure error. To obtain a sufficient number of adsorption points close to zero exposure for the clean surface and for low K coverages, low methane pressures (of the order of tenths of millibars) were used. In these cases, the thermal finger, heated to the sample temperature, was placed close to the sample surface (<1 mm) to ensure that the effective temperature of the gas molecules hitting the surface was equal to the surface temperature (20).

3. EXPERIMENTAL RESULTS

3.1. Initial Sticking Coefficients

Figure 1 shows some of the results obtained for methane chemisorption on Ni(100) without and with predeposited potassium versus the logarithm of the methane exposure (measured in ML, i.e., number of CH_4 molecules hitting the surface per surface nickel atom). Figure 2 shows similar results obtained for Ni(111). An impression of the reproducibility of the results can be gained from the two sets of results shown for the initially clean Ni(111) surface. The initial sticking coefficients are determined by the slope at zero exposure of an adsorption model fitted to the chemisorption results. The model used for the Ni(100) results corresponds to blocking of the adsorption site and the nearest neighbor sites. This model, which was used previously to derive initial sticking coefficients from methane chemisorption results on clean Ni(100) (4, 20), has been shown to give a good description of the Ni(100) chemisorption results at least up to a carbon coverage of 0.3 ML (20). However, it does not give a good description of the Ni(111) chemisorption results, as indicated by the different appearances of the results in Fig. 1 and 2. However, in agreement with Holmblad *et al.* (28), it is found that a first order Langmuir expression gives a satisfactory fit to the experimental results on Ni(111). The fact that these models are convenient for the determinations of the initial sticking coefficients does not prove, however, that the atomic behavior implied by the models are faithful descriptions of reality. Other mathematical functions might be quite as useful for this purpose. Figures 3 and 4 show the initial sticking coefficients derived from the 475 and 500 K results, respectively. The horizontal error bars are reflecting the spread of the $R_{K,Ni}$ values measured simultaneously with the points of the methane chemisorption curve.

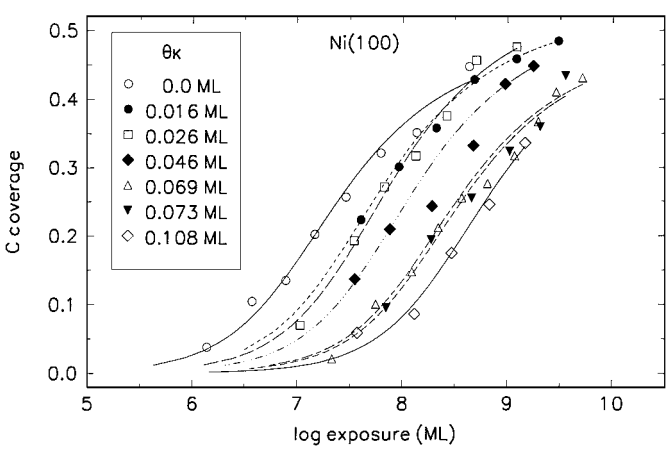

FIG. 1. CH_4 chemisorption on Ni(100) vs methane exposure (ML) (logarithmic scale) at 500 K. Potassium coverages: 0.0 ML (○), 0.016 ML (●), 0.026 ML (□), 0.046 ML (◆), 0.069 ML (△), 0.073 ML (▼), and 0.108 ML (◇). The curves are calculated using the nearest neighbors blocking model described in the text.

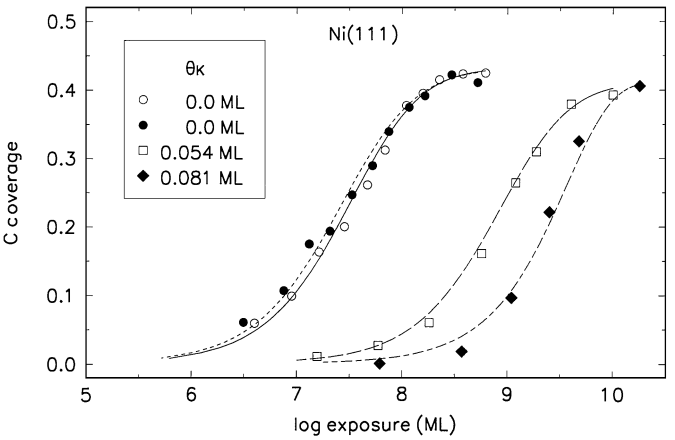

FIG. 2. CH_4 chemisorption on Ni(111) vs methane exposure (ML) (logarithmic scale) at 500 K. Potassium coverages: 0.0 ML (○), 0.0 ML (●), 0.054 ML (□), and 0.081 ML (◆). The curves are calculated using the Langmuir model described in the text.

3.2. Carbon Saturation Coverage

Some of the methane chemisorption measurements, plotted in logarithmic scale in Figs. 1 and 2, were continued close

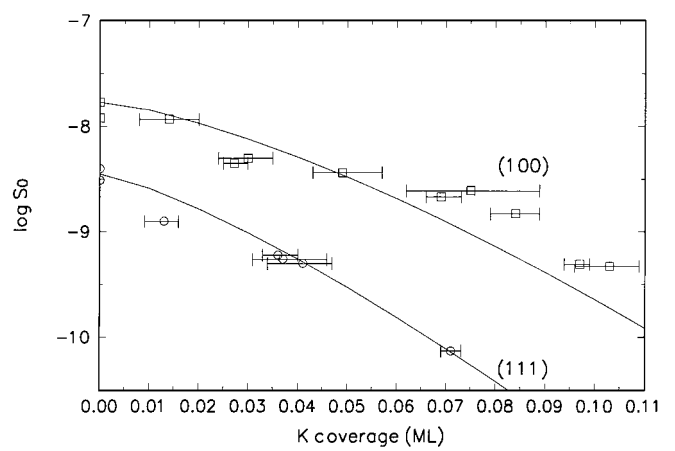

FIG. 3. The initial sticking coefficient, s_0 (logarithmic scale), for CH_4 chemisorption on Ni(100) (□) and Ni(111) (○) at 475 K vs potassium coverage. The solid lines are guides to the eyes.

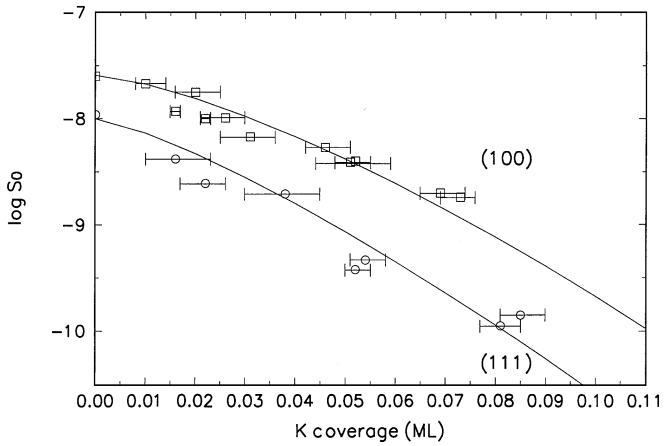

FIG. 4. Same as Fig. 3, but for CH_4 chemisorption at 500 K.

to saturation. It turns out that the carbon saturation coverage is influenced very little by the potassium coverage in the range considered, i.e., 0–0.12 ML, in contrast to the initial sticking coefficient. Also C_2H_4 adsorption at 475 K with 0.1 ML potassium preadsorbed resulted in almost the same carbon saturation coverage as without potassium. Experiments with the opposite order of deposition showed that carbon saturation did not prevent K deposition.

4. DENSITY FUNCTIONAL THEORY CALCULATIONS

4.1. Calculational Details

The self-consistent DFT calculations were performed using the generalized gradient approximation (GGA) to describe exchange and correlation effects (29, 34). The ionic cores are described by ultrasoft pseudo-potentials (30) generated within the PW91 approximation. The electron density is determined self-consistently by iterative diagonalization of the Kohn–Sham Hamiltonian, Fermi population of the Kohn–Sham states ($k_BT = 0.1$ eV), and Pulay mixing of the electronic density (31). Plane waves with a kinetic cutoff at 25 Ry are used to expand the wave functions. All total energies are extrapolated to zero electronic temperature. In each case we used the PW91 exchange-correlation functional in the self-consistent determination of the electron density and then calculated the total energy using the more accurate RPBE functional (34). Due to the variational property of the total energy functional, this gives rise to marginal errors compared to a calculation using the RPBE functional all the way through (34).

The Ni surfaces are modeled by a periodic array of slabs separated by ∼9 Å of vacuum. Rigid Ni slabs in the bulk geometry are used to represent the substrates with the calculated lattice constant $a_0 = 3.5182$ Å. The results are for two layer slab calculations except for test runs using four layer slabs for single points as indicated below. (2×2) and (2×4) surface unit cells were used giving CH_4 coverages of 0.25 and 0.125 ML respectively. The Brillouin zones were sampled by 18 (16) and 8 (8) $\vec{k}$ points (number of Ni(100) points in paranthesis).

TABLE 1

Selected Bond Distances and Angles for the Transition State

	Ni(111)	Ni(100)
C–H1 (Å)	1.59	1.59
C–H2 (Å)	1.10	1.10
C–H3 (Å)	1.10	1.10
C–H4 (Å)	1.10	1.10
C–Ni (Å)	2.08	2.05
H1–C–H2 (°)	71.0	73.2
H3–C–H4 (°)	115.4	116.2
H2–C–H3 (°)	112.0	112.3
H2–C–H4 (°)	111.8	112.3
α (°)	84.4	83.0
θ (°)	52.0	52.8

4.2. Results

The transition state for dissociation of methane on Ni(111) has previously been characterized by density functional theory calculations (32). Using the reported transition state geometry as a starting point for calculations, values for the dissociating C–H bond length were chosen whereas the remaining degrees of freedom of the methane molecule were allowed to relax. Using this approach to sample the potential energy surface around the reported transition state it was possible to localize the saddle point. The geometry of the transition state given in Table 1 is in good agreement with the work by Kratzer *et al.* (32). The interaction energy for selected configurations is given in Fig. 5

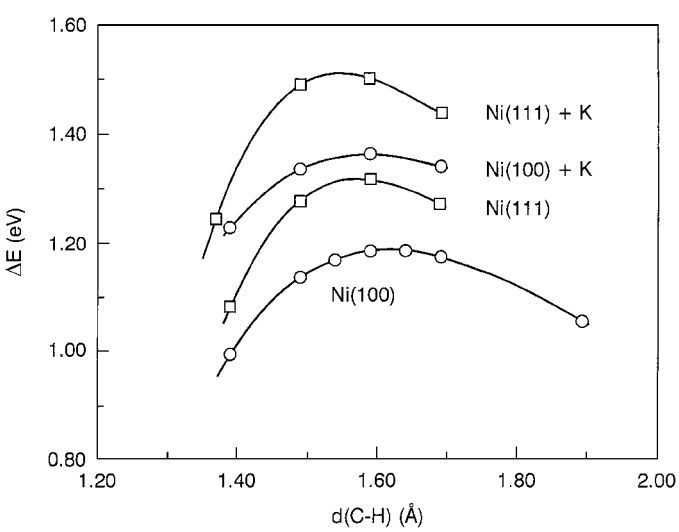

FIG. 5. ΔE vs C–H bond length for Ni(100) and Ni(111) without and with 0.125 ML potassium coverage, where ΔE is calculated in accordance with Eq. [1].

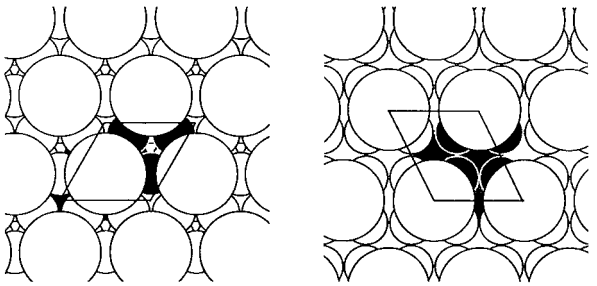

FIG. 6. (2×2) surface unit cells with one K atom in the cell. Left, Ni(111); right, Ni(100).

where

$$\Delta E = E_{\mathrm{TOT(Ni,CH_4)}} - E_{\mathrm{TOT(Ni)}} - E_{\mathrm{TOT(CH_4,isolated)}}. \quad [1]$$

For the Ni(100) surface, the same approach was used and the calculated energies are included in Fig. 5 and the geometry for the saddle point in Table 1. A comparison of the two geometries shows many similarities and for both surfaces, the dissociation takes place on top of a surface Ni atom. The dissociating C–H bond forms an angle of 52.0° and 52.8° with the surface normal through carbon for Ni(111) and Ni(100), respectively. The bond is stretched from the bond length of 1.09 Å in the isolated CH_4 molecule to 1.59 Å in the transition state. The distances from C to the surfaces are 2.08 and 2.05 Å.

The next step is to investigate the effect of potassium. The position of potassium on the surfaces is first optimized using (2×2) lateral unit cells and two layer slabs. The Ni atoms are kept in the bulk geometry with no relaxation or reconstruction. For Ni(111), the ontop position of K is slightly favored with a distance of 2.81 Å to the surface, whereas K on Ni(100) prefers the fourfold hollow site 2.70 Å from the surface (Fig. 6). For both surfaces the distances and positions agree very well with experiments (27, 35, 36).

The (2×2) unit cell is too small for investigations of the effect of coadsorbed potassium on the energy barriers. Therefore, calculations with one K and one CH_4 atom in the (2×4) lateral unit cells (Fig. 7) were performed. The potassium atoms are given the positions determined previously whereas for CH_4 the dissociating C–H bond is given fixed values and the rest of the degrees of freedom of methane are allowed to relax. The energies for fixed C–H bond distances calculated using Eq. [1] are given in Fig. 5. For the two surfaces the effect of potassium on the transition state energy has about the same magnitude. Potassium increases the transition state energy and thus has a deactivating effect as observed experimentally.

We have checked that the methane–surface interaction energy at the transition state only depends marginally on the size of the unit cell. Calculations for the (2×4) unit cell without K give energy barriers that are lowered by 19 and 23 meV for Ni(100) and Ni(111), respectively, compared to the (2×2) unit cells. Using the results for the (2×4) unit cells, the effect of coadsorbing potassium on the energy barriers is 0.20 eV for Ni(100) and 0.21 eV for Ni(111). The effects of using more layers in the calculation have also been tested. A calculation with the dissociating C–H bond distance fixed to 1.59 Å on a four-layer slab in the bulk geometry of the the (111) facet gives a relative energy of this complex, where the rest of the methane degrees of freedom are relaxed, which is 36 meV higher than for the corresponding two-layer calculation. We conclude on this basis that the error introduced by using only two layers is quite small.

An analysis of the dipole moment of the transition state complex without coadsorbed potassium

$$\mu = \int d\vec{r}\, \Delta\rho_{\mathrm{TS}}(\vec{r}) z, \quad [2]$$

with $\Delta\rho_{\mathrm{TS}}(\vec{r}) = \rho_{\mathrm{TS}}^{\mathrm{CH_4/Ni}} - \rho^{\mathrm{Ni}}$ shows that for both surfaces the transition state complexes have significant dipole moments (Table 2). When a dipole with dipole moment μ interacts with an electric field ε, the interaction energy is

$$\Delta E = -\varepsilon\mu. \quad [3]$$

We have calculated the maximum magnitude of the electric field induced by potassium, $\varepsilon_{\mathrm{K}}^{\mathrm{max}}$, outside the surface from the potassium-induced electrostatic potential $\Delta\phi_{\mathrm{K}} = \phi_{\mathrm{K/Ni}} - \phi_{\mathrm{Ni}}$ along a line perpendicular to the surface and through the site of adsorption as described by Mortensen *et al.* (37). The values for $\varepsilon_{\mathrm{K}}^{\mathrm{max}}$ are given in Table 2. The product $\varepsilon_{\mathrm{K}}^{\mathrm{max}}\mu_{\mathrm{TS}}$ and the self-consistently

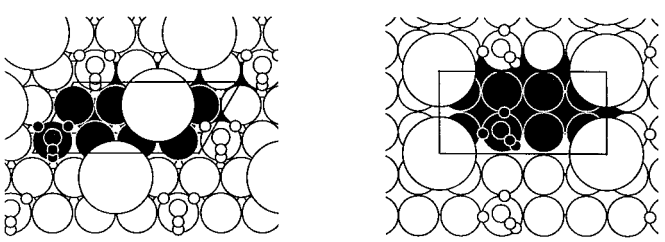

FIG. 7. (2×4) surface unit cells with one K atom and one CH_4 molecule in the cell. Left, Ni(111); right, Ni(100).

TABLE 2

Induced Dipole Moments and K-Induced Fields

	Ni(111)	Ni(100)
Induced dipole moments μ_{TS} (eÅ)	0.20	0.19
K-induced field		
$\varepsilon_{\mathrm{K}}^{\mathrm{max}}$ (V/Å)	−1.05	−0.89
$\varepsilon_{\mathrm{K}}^{\mathrm{max}}\,\mu_{\mathrm{TS}}$	−0.21	−0.17
$\Delta E^{\mathrm{TS}} = E_{\mathrm{Ni,K}}^{\mathrm{TS}} - E_{\mathrm{Ni}}^{\mathrm{TS}}$(eV)	0.21	0.20

calculated ΔE_{TS} are also shown in Table 2. It is seen that the absolute values of the two quantities not only show the same trend when going from Ni(111) to Ni(100) but they are also of the same magnitude. This indicates that the deactivating effect of potassium is dominated by the simple electrostatic interaction between adsorbed potassium and the transition state complex.

5. DISCUSSION

The amount of CH_4 chemisorbed on the nickel surface is, as in previous studies (4), determined by measuring the area of the XPS C 1*s* peak. The measurement does not distinguish between carbon from the various possible surface species, which may be present after chemisorption and dehydrogenation of CH_4. It is known, however, that at the temperatures of the present experiments only C and CH are left on the surface (38).

The present measurements of the very small sticking probabilities in the range from about 5×10^{-8} to below 10^{-10} clearly show that small amounts of preadsorbed potassium have a strong inhibiting effect on the chemisorption of CH_4 on Ni(100) and Ni(111). The initial sticking coefficient of CH_4 on Ni(100) at 475 and 500 K decreases by a factor of about 6 when the potassium coverage changes from 0 to 0.05 ML and by a factor of about 12 on Ni(111) for the same potassium coverage change. These changes are far stronger than any simple blocking model predicts. The factor should be 1.05 if only one site is blocked for each adsorbed K atom, while if also nearest neighbor sites are blocked for each randomly deposited K atom the theoretical factor is 1.3 for the (100) and 1.1 for the (111) surface (4, 39, 40). If also next nearest neighbor sites are blocked the further increase of the factor amounts to only a few percent (40). The change of the CH_4 dissociation barrier of about 19 kJ/mol, when 0.125 ML potassium is deposited on Ni(100) or Ni(111) as obtained by present DFT–GGA calculations, is in good agreement with this strong inhibition. Even the absolute magnitude of the calculated effect is reasonable compared to the experiments. An increase in barrier of $\Delta E_{TS} = 19$ kJ/mol should result in a decrease of the sticking probability of the order $\exp(-\Delta E_{TS}/kT) = 0.01$ at 500 K. This is in good agreement with what is found by extrapolating the experimental results in Fig. 3 and 4 to a K coverage of 0.125 ML.

The close agreement between the energy of the methane dipole moment in the field induced by the K adatoms and the calculated change of barrier strongly support the suggestion that also in the present chemisorption system electrostatic interactions can account for the observed influence of alkali (15, 16). It may be surprising that methane in the transition state gives rise to a relatively large dipole moment. The reason is that the closed shell activated complex interacts repulsively with the electrons of the surface. This means that the surface electrons are pushed closer toward the surface, giving rise to a net electron transfer toward the surface. Thus the picture is different from the interaction between, e.g., adsorbed potassium and adsorbed CO or N_2 molecules, where the adsorbate dipole moment is due to an electron transfer from the surface into the antibonding orbitals of the molecule (15, 16).

We note that since the poisoning effect of potassium on methane dissociation is due to the electrostatic field of the potassium interacting with the induced dipole moment of the methane transition state complex, the effect is far from restricted to the geometries studied here. Any form of the potassium where there is a net electron transfer toward the surface will give rise to such an electric field and thus to the poisoning. This includes cases where potassium is coadsorbed with, e.g., oxygen or carbon. Other electropositive adsorbates like Na, Cs, or Mg should give rise to the same effect. The effect will also include methane dissociating at, e.g., defects, because the repulsion between the surface electrons and the transition state complex pushing electrons toward the surface will still be present. The fact that the poisoning effect can be explained by a simple electrostatic model thus allows us to suggest that the effect is very general.

6. SUMMARY

The dissociative chemisorption of methane on Ni(100) and Ni(111) with preadsorbed potassium in the range 0–0.12 ML has been measured at 475 and 500 K. The potassium adatoms, in the coverage range investigated, have very little influence on the saturation carbon coverage after high methane exposures, but they have a strong inhibiting effect on the initial sticking probability.

The experimental results are interpreted by means of self-consistent density functional theory (DFT–GGA) calculations. They show that the barrier for dissociation of CH_4 is increased by 0.21 and 0.20 eV when 0.125 ML potassium is preadsorbed on Ni(111) and Ni(100), respectively. They also show that in the transition state of CH_4 dissociation, a dipole moment of 0.20 and 0.19 eÅ is induced in the Ni(111) and the Ni(100) surface, respectively. The product of this dipole moment and the maximum value of the field induced by the potassium adatoms is in excellent agreement with the calculated change of the barrier when potassium is preadsorbed, suggesting that the inhibition is mainly determined by an electrostatic interaction.

ACKNOWLEDGMENTS

P. Kratzer is gratefully acknowledged for helpful discussions. The authors thank M. S. Madsen and J. Gottschalck for assistance with some of the measurements. This work was supported by the Danish Research Councils through the Interdisciplinary Research Center for Catalysis (ICAT). The Center for Atomic-scale Materials Physics (CAMP) is sponsored by the Danish National Research Foundation.

REFERENCES

1. Lee, M. B., Yang, Q. Y., Tong, S. L., and Ceyer, S. T., *J. Chem. Phys.* **87**, 2724 (1987).
2. Hamza, A. V., and Madix, R. J., *Surf. Sci.* **179**, 25 (1987).
3. Beebe, T. B., Jr., Goodman, D. W., Kay, B. D., and Yates, J. T., Jr., *J. Chem. Phys.* **87**, 2305 (1987).
4. Chorkendorff, I., Alstrup, I., and Ullmann, S., *Surf. Sci.* **227**, 291 (1990).
5. Holmblad, P. M., Wambach, J., and Chorkendorff, I., *J. Chem. Phys.* **102**, 8255 (1995).
6. Swang, O., Faegri, J. K., Gropen, O., Wahlgren, U., and Siegbahn, P. E. M., *Chem. Phys.* **156**, 379 (1991).
7. Yang, H., and Whitten, J. L., *J. Chem. Phys.* **96**, 5529 (1992).
8. Burghgraef, H., Jansen, A. P. J., and van Santen, R. A., *J. Chem. Phys.* **101**, 11012 (1994).
9. Rostrup-Nielsen, J. R., *in* "Catalysis, Science and Technology" (J. R. Andersson and M. Boudart, Eds.), Vol. 5, Chapter 1. Springer-Verlag, Berlin, 1984.
10. Bonzel, H. P., and Pirug, G., *in* "The Chemical Physics of Solid Surfaces" (D. A. King and D. P. Woodruff, Eds.), Vol. 6, Chapter 3. Elsevier, Amsterdam, 1993.
11. Bowker, M., *in* "The Chemical Physics of Solid Surfaces" (D. A. King and D. P. Woodruff, Eds.), Vol. 6, Chapter 7. Elsevier, Amsterdam, 1993.
12. Joyner, R. W., *in* "The Chemical Physics of Solid Surfaces" (D. A. King and D. P. Woodruff, Eds.), Vol. 6, Chapter 8. Elsevier, Amsterdam, 1993.
13. Kiskinova, M. P., "Poisoning and Promotion in Catalysis Based on Surface Science Concepts and Experiments," Stud. Surf. Sci. Catal., Vol. 70. Elsevier, Amsterdam, 1992.
14. Bonzel, H. P., Bradshaw, A. M., and Ertl, G. (Eds.), "Physics and Chemistry of Alkali Metal Adsorption," Materials Science Monographs, Vol. 57. Elsevier, Amsterdam. 1989.
15. Nørskov, J. K., Holloway, S., and Lang, N. D., *Surf. Sci.* **137**, 65 (1984).
16. Nørskov, J. K., *in* "The Chemical Physics of Solid Surfaces" (D. A. King and D. P. Woodruff, Eds.), Vol. 6, Chapter 1. Elsevier, Amsterdam, 1993.
17. Müller, J. E., *in* "The Chemical Physics of Solid Surfaces" (D. A. King and D. P. Woodruff, Eds.), Vol. 6, Chapter 2. Elsevier, Amsterdam, 1993.
18. Ceyer, S. T., Yang, Q. Y., Lee, M. B., Beckerle, J. D., and Johnson, A. D., *Stud. Surf. Sci. Catal.* **36**, 51 (1988).
19. Rostrup-Nielsen, J. R., and Christiansen, L. J., *Appl. Catal A* **126**, 381 (1995).
20. Nielsen, B. Ø., Luntz, A. C., Holmblad, P. M., and Chorkendorff, I., *Catal. Lett.* **32**, 15 (1995).
21. Shirley, D. A., *Phys. Rev. B* **5**, 4709 (1972).
22. Tougaard, S., *Surf. Sci.* **216**, 343 (1989).
23. Tokutaka, H., Ishihara, N., Nishimori, K., Kishida, S., and Isomoto, K., *Surf. Interface Anal.* **18**, 697 (1992).
24. Onuferko, J. H., Woodruff, D. P., and Holland, B. W., *Surf. Sci.* **87**, 357 (1979).
25. Klink, C., Stensgaard, I., Besenbacher, F., and Lægsgaard, E., *Surf. Sci.* **342**, 250 (1995).
26. Fisher, D., and Diehl, R. D., *Phys. Rev. B* **46**, 2512 (1992).
27. Kaukasoina, P., Lindroos, M., Diehl, R. D., Fisher, D., Chandavarkar, S., and Collins, I. R., *J. Phys. Condens. Matter* **5**, 2875 (1993).
28. Holmblad, P. M., Larsen, J. H., and Chorkendorff, I., *J. Chem. Phys.* **104**, 7289 (1996).
29. Perdew, J. P., Chevary, J. A., Vosko, S. H., Jackson, K. A., Pederson, M. R., Singh, D. J., and Fiolhais, C., *Phys. Rev. B* **46**, 6671 (1992).
30. Vanderbilt, D., *Phys. Rev. B* **41**, 7892 (1990).
31. Kresse, G., and Furthmüller, J., *Comput. Mat. Sci.* **6**, 15 (1996).
32. Kratzer, P., Hammer, B., and Nørskov, J. K., *J. Chem. Phys.* **105**, 5595 (1996).
33. Mavrikakis, M., Hammer, B., and Nørskov, J. K., *Phys. Rev. Lett.* **81**, 2819 (1998).
34. Hammer, B., Hansen, L. B., and Nørskov, J. K., *Phys. Rev. B* **59**, 7413 (1999).
35. Wedler, H., Mendez, M. A., Bayer, P., Löffler, U., Heinz, K., Fritzsche, V., and Pendry, J. B., *Surf. Sci.* **293**, 47 (1993).
36. Davis, R., Hu, X. M., Woodruff, D. P., Weiss, K. U., Dippel, R., Schindler, K. M., Hofmann, Ph., Fritzsche, V., and Bradshaw, A. M., *Surf. Sci.* **307–309**, 632 (1994).
37. Mortensen, J. J., Hammer, B., and Nørskov, J. K., *Surf. Sci.* **414**, 315 (1998).
38. Yang, Q. Y., and Ceyer, S. T., *J. Vacuum Sci. Technol. A* **6**, 851 (1988).
39. Andersen, N. T., Topsøe, F., Alstrup, I., and Rostrup-Nielsen, J. R., *J. Catal.* **104**, 454 (1987).
40. Alstrup, I., and Andersen, N. T., *J. Catal.* **104**, 466 (1987).